Subunit topology of the *Rhodococcus* proteasome

Frank Zühl[a], Tomohiro Tamura[a], Iztok Dolenc[a], Zdenka Cejka[a], István Nagy[b], René De Mot[b], Wolfgang Baumeister[a,*]

[a] *Max-Planck-Institute for Biochemistry, D-82152 Martinsried, Germany*
[b] *F.A. Janssens Laboratory of Genetics, Catholic University of Leuven, B-3001 Heverlee, Belgium*

Received 11 November 1996; revised version received 18 November 1996

Abstract The 20S proteasome, isolated from the nocardioform actinomycete *Rhodococcus erythropolis* strain NI86/21, is built from two α-type and two β-type subunits. In order to probe the subunit topology, we have set up an expression system which allows coexpression of the genes encoding the α- and β-subunits in all possible combinations. The four respective constructs obtained yielded fully assembled and proteolytically active proteasomes. Biochemical, kinetic and electron microscopy analysis allow us to rule out several of the models which were originally envisaged for the subunit topology of the *Rhodococcus* proteasome. The experiments further indicate that the assembly pathways of the *Rhodococcus* and of the *Thermoplasma* proteasome differ in some important details.

Key words: Proteasome; Proteolysis; *Rhodococcus*; Gene expression

1. Introduction

The 20S proteasome is a macromolecular assembly designed to confine its potentially dangerous proteolytic activity to an inner cavity. Access to this cavity is restricted to unfolded proteins [1]. Therefore, the proteasome is functionally linked to a substrate recognition and unfolding machinery [2]. In eukaryotic cells this is provided by the 19S or 'cap' complex which associates with the 20S core to form the 26S proteasome [3]. This 26S complex is able to degrade ubiquitinated proteins in an ATP-dependent manner (see [4–7]).

Until 20S proteasomes were discovered in the archaeon *Thermoplasma* [8] it seemed that the occurrence of proteasomes was restricted to eukaryotic cells. The *Thermoplasma* proteasome is built from two different but related subunits, α and β, which collectively form a barrel-shaped complex. Two seven-membered rings of β-subunits form the core of the complex and the central cavity where the active sites are located. The core is flanked by two seven-membered rings of α-subunits jointly creating two 'antechambers' with the β-subunits. The α-subunits 'chaperone' the folding, processing and assembly of the β-subunits and they define the polypeptide channel which controls access to the interior of the proteasome. The *Thermoplasma* proteasome has, because of its relative simplicity, taken a pivotal role in elucidating the structure of the proteasome [9], its enzymatic mechanism [10], assembly and posttranslational processing [11,12].

Although the quaternary structure of eukaryotic 20S proteasomes is basically the same [13], their subunit composition is much more complex. The eukaryotic complex is formed by two copies each of 14 different although related subunits which can be divided into two subgroups reflecting their relationship to either the α- or the β-subunit of the archaeal proteasome [14].

More recently, a database search revealed the existence of β-type but not α-type proteasomal subunits in some eubacteria [15]. Since the gene encoding the β-type subunit in *E. coli* was found in an operon (*hslVU*) with a gene encoding an ATPase belonging to the HSP100/Clp family, it was suggested that a hybrid complex exists, which combines features of the ClpAP system and the proteasome [15,16]. Recent structural studies of *E. coli* HslVU have substantiated this proposal: HslV, the proteolytic component which is distantly related to the β-subunit of the *Thermoplasma* proteasome, forms the proteolytic core of two hexameric rings; the ATPase (HslU) forms homooligomeric rings which associate directly with the HslV core, reminiscent of the organisation of ClpAP (Rohrwild et al., submitted).

Recently we have shown that other bacteria possess genuine proteasomes, composed of α- and β-subunits [17]. Surprisingly, proteasomes isolated from the actinomycete *Rhodococcus erythropolis* strain NI86/21 contained two α-type and two β-type subunits. The corresponding genes were found to be arranged in two separate operons, $prcB_1A_1$ and $prcB_2A_2$. Since the two operons differ significantly in G+C content it appears more likely that one of them originates from a relatively recent horizontal gene transfer event rather than from a gene duplication. The occurrence of proteasomes built from two α- and two β-type subunits appears to be the exception rather than the rule amongst the actinomycetes (De Schrijver et al., submitted). Although the *Rhodococcus* proteasome appears on electron micrographs to be very similar to the *Thermoplasma* proteasome, the structural data available so far did not allow us to propose a unique model for the complex, the more since we were uncertain about its symmetry [17]. Although all archaeal or eukaryotic proteasomes studied so far have 7-fold or pseudo-7-fold symmetry, respectively, this must not necessarily hold for bacterial proteasomes. Indeed, the rings formed by HslV are of 6-fold symmetry (Rohrwild et al., submitted). Several models for the subunit topology of the *Rhodococcus* proteasome must be taken into consideration (Fig. 1). Model I assumes that two distinct subpopulations of proteasomes exist, one formed by α_1 and β_1 (the products of the $prcB_1A_1$ operon) and the other formed by α_2 and β_2 (the products of the $prcB_2A_2$ operon). A priori both 6-fold and 7-fold symmetric complexes could exist.

*Corresponding author. Fax: (49) (89) 8578 2641.
E-mail: zuehl@vms.biochem.mpg.de

Abbreviations: SDS, sodium dodecyl sulfate; PAGE, polyacrylamide gel electrophoresis; DMSO, dimethylsulfoxide; DTT, dithiothreitol; AMC, 7-amino-4-methylcoumarin; Suc, succinyl; Z, benzoxycarbonyl; Boc, *N-t*-butoxycarbonyl; Bz, benzonyl; MW, molecular weight.

PII S0014-5793(96)01403-2

The same is true for model II which suggests that four different homooligomeric rings formed by α_1, α_2, β_1 and β_2 are stacked together to form a single complex. Assuming that, as in all other proteasomes studied so far, the two α-subunits form the outer and the two β-subunits form the inner rings, two variants are possible which differ in the stacking along the cylinder axis. In both cases the dyad axis which is characteristic of archaeal and eukaryotic proteasomes would vanish.

In model III, the two α- and two β-subunits are incorporated, in an alternating fashion, into heterooligomeric rings. This model requires an even number of subunits per ring and shows a pseudo-6-fold symmetry. The stoichiometry of the two α-type and two β-type subunits isolated from *Rhodococcus* is indeed close to 1:1. Finally, model IV proposes a stochastic distribution of the two types of subunits within the α- and β-rings. Given the high degree of similarity (α_1 and α_2 are 81.6%, β_1 and β_2 are 86.5% identical) such promiscuity cannot be ruled out.

In order to address the issue of subunit topology and to narrow down the number of possible models, we have set up an expression system which allows coexpression of the four proteasomal genes in all possible combinations. This also provides the basis for more detailed in vitro studies aimed at elucidating the assembly pathway and the mechanisms involved in it. In this context the complexity of the *Rhodococcus* complex, which is intermediate between the eukaryotic and the other prokaryotic proteasomes studied so far, is obviously advantageous.

2. Materials and methods

2.1. Purification of proteasomes from Rhodococcus

The nocardioform actinomycete strain NI86/21 was recently identified as an *R. erythropolis* strain based on chemotaxonomical and 16S rRNA sequence data (De Schrijver et al., submitted). For the isolation of proteasomes, *R. erythropolis* NI86/21 obtained from the National Collection of Agricultural and Industrial Microorganisms (NCAIM, Budapest) was grown in Luria broth at 30°C. The isolation and purification of the 20S proteasome were carried out as described previously [17] using a sequence of chromatographic steps starting with Sepharose 6B gel filtration chromatography followed by DEAE-Sephacel ion exchange chromatography, a hydroxyapatite affinity column, and finally FPLC ion exchange chromatography (MonoQ, Pharmacia) plus an additional gel filtration step (Superose 6 HR, Pharmacia). Column fractions were assayed for chymotryptic activity using the fluorogenic peptide substrate Suc-Leu-Leu-Val-Tyr-7-AMC (Bachem, Heidelberg). The purity of the collected proteasomes was analyzed using 16% Tricine-SDS PAGE [18]. Protein concentration was determined by the Bradford protein assay (BioRad) as described [19].

2.2. Cloning the genes encoding the four subunits of the Rhodococcus proteasome

The templates used for PCR amplification of the proteasome genes were pFAJ2471 for the β_1-α_1-subunits, and pFAJ2466 for the β_2-α_2-subunits. pFAJ2466 contained a 1.8 kb *Pst*I fragment of λFAJ2029 [17] subcloned in pUC18. By partial *Bgl*II digestion of λFAJ2030 [20] a 2.6 kb fragment was recovered with the complete β_2-α_2 coding regions. This fragment was subcloned in *Bam*HI-digested pUC18 to generate pFAJ2471. We used the low copy expression vector pT7-7 [21] containing a T7 promotor followed by an *E. coli* Shine Dalgarno sequence and a multiple cloning site. The constructs generated are summarized in Fig. 2.

2.3. pT7-7β_1 and pT7-7β_2

To perform expression cassette PCR (EC-PCR) four primers were designed for the amplification of the two β-subunit encoding genes. Two different unique restriction sites (*Nde*I and *Eco*RI) as well as a sequence which encodes six consecutive histidine residues ($(His)_6$) at the C-terminus of both β-genes and therefore facilitates purification of the recombinant proteins, were added to the 5′ ends of the PCR primer. PCR was performed with pFAJ2466 and pFAJ2471 as templates in a Perkin Elmer Cetus 480 thermocycler, using *Pfu* DNA polymerase (Stratagene). All PCR primers were synthesized on a 380A DNA synthesizer (Applied Biosystems). After sequential digestion with the corresponding enzymes, the PCR fragments were cloned into pT7-7 yielding pT7-7β_1 and pT7-7β_2, respectively. Screening and propagation of the plasmids were carried out using the *E. coli* strain XL1-Blue (Stratagene). All transformations were performed by electroporation (*E. coli* Pulser, BioRad). The accuracy of the reading frames was confirmed by DNA cycle sequencing (373A DNA Sequencer) using the DyeDeoxy Terminator Cycle Sequencing kit (Applied Biosystems).

2.4. pT7-7$\beta_1\alpha_1$, pT7-7$\beta_2\alpha_2$, pT7-7$\beta_1\alpha_2$ and pT7-7$\beta_2\alpha_1$

For coexpression of the two α- and the two β-subunit genes in various combinations, we amplified the two α-subunit encoding genes in the same way as described before for β. For this purpose, four PCR primers containing two additional unique restriction sites (*Pst*I, *Hin*dIII) at the 5′ end were designed. Additionally, a Shine-Dalgarno sequence and an 8-base-pair translational spacer element preceding the start codon of the α-genes were inserted. After performing PCR, fragments were digested with the appropriate enzyme and inserted downstream of the β-genes in the expression vectors pT7-7β_1 and pT7-7β_2 to obtain the four constructs III–VI in Fig. 2.

2.5. pT7-7α_1(H) and pT7-7α_2(H)

In order to express the α-subunits separately, the α-genes were amplified by PCR using primers which were flanked by unique restriction sites (*Nde*I and *Eco*RI for α_1, *Nde*I and *Bam*HI for α_2) and additionally contained a $(His)_6$ tag at the C-terminus. The PCR products were digested and cloned into pT7-7 to obtain pT7-7α_1(H) and pT7-7α_2 (H) (Fig. 2, VII and VIII).

2.6. pT7-7α_1(H)α_2 and pT7-7α_2(H)α_1

For the combined expression of both α-subunits, with only one of them carrying a $(His)_6$ tag, we removed the β-genes from the expression constructs pT7-7$\beta_1\alpha_1$ and pT7-7$\beta_2\alpha_2$ by cutting with *Nde*I and *Pst*I. Similarly, we digested the plasmids pT7-7α_1(H) and pT7-7α_2(H) with *Nde*I and *Pst*I to obtain the α-genes containing the $(His)_6$ tag at their C-termini. Ligation of the $\alpha_1(His)_6$ fragment into the pT7-7α_2 vector fragment and the $\alpha_2(His)_6$ fragment into the pT7-7α_1 vector fragment resulted in the two mixed constructs pT7-7α_1(H)α_2 and pT7-7α_2(H)α_1 (Fig. 2, IX and X).

2.7. Expression and purification of the recombinant proteins

For expression, BL21 (DE3) cells (Stratagene) were transformed and grown in LB medium to mid-log phase at 30°C. After induction with 1 mM isopropyl-β-D-thiogalactopyranoside (IPTG) for 5 h, cells were harvested and resuspended in sonication buffer (50 mM Na-phosphate, 300 mM NaCl, pH 8), treated for 40 min on ice with lysozyme (1 mg/ml, Sigma) and sonicated for 10 min (Sonifier 250, Branson).

The lysate was further fractionated by centrifugation (30 000×*g*, 1 h) and the supernatant was loaded directly on a Ni-NTA affinity column (0.65×4 cm, Qiagen), previously equilibrated with sonication buffer. Tagged proteins were eluted with a gradient of 0–500 mM imidazole. Fractions were analyzed by 16% Tricine SDS-PAGE and assayed for proteolytic activity. Fractions containing the pure protein were pooled and dialyzed against 50 mM Tris, 1 mM DTT, pH 7.5.

2.8. Peptidase assays and kinetic analysis

All synthetic fluorogenic peptides (Bachem, Heidelberg) were dissolved in DMSO. The determination of the kinetic parameters of Suc-LLVY-AMC hydrolysis was performed using a Contron SFM 25 fluorescence spectrophotometer with a jacketed cell holder which allowed adjustment of the reaction temperature to 37.0±0.1°C by a circulating water bath. After equilibration of 280 μl assay buffer (10 mM Tris-HCl, 1 mM EDTA, 1 mM NaN_3, pH 7.5) with the given substrate concentration (10–1000 μM, 5% final concentration DMSO) at 37°C, 0.5 μg of the purified enzyme (20 μl) was added and the reaction mixture was immediately loaded into the cuvette. Reaction progress was monitored at excitation and emission wavelengths of 360 and 460 nm, respectively. During the assay, less than 5% of the sub-

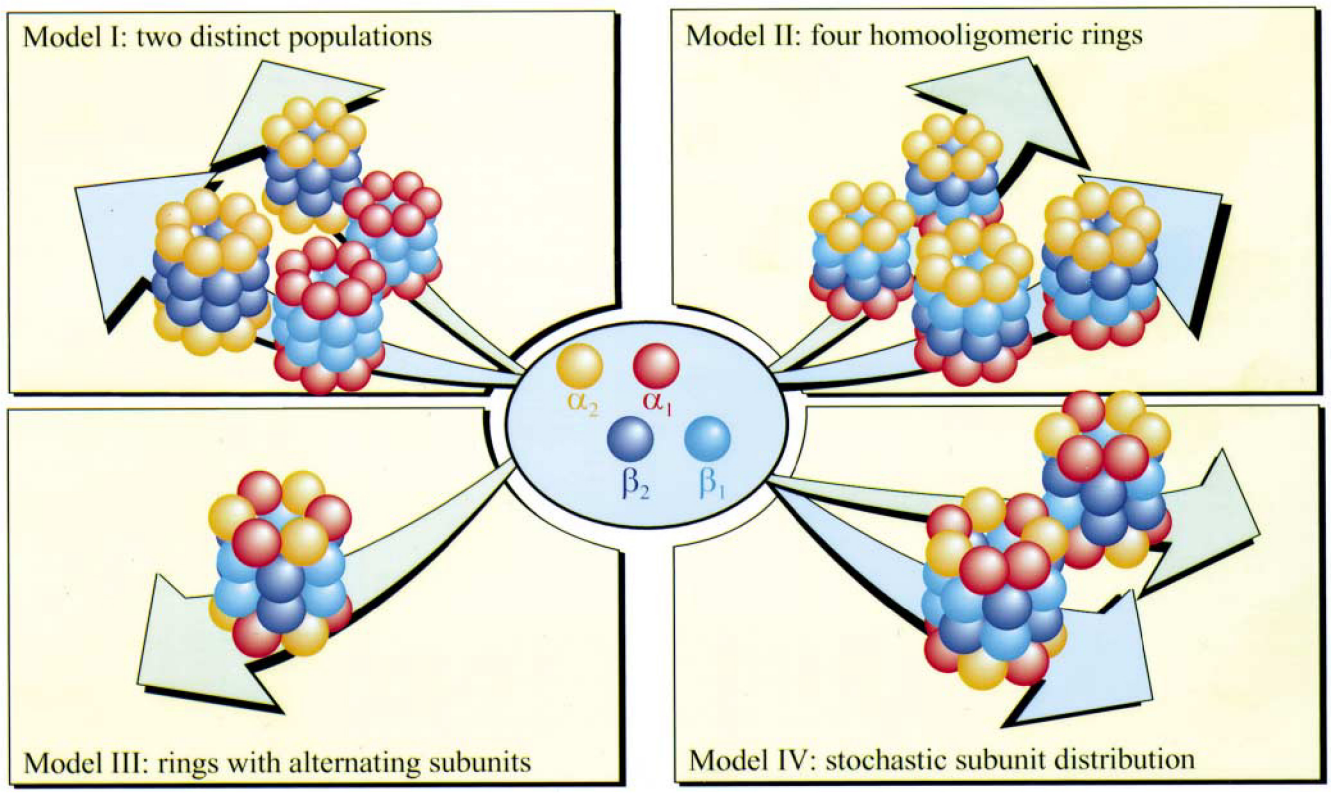

Fig. 1. Synopsis of possible subunit topologies in the *Rhodococcus* proteasome.

strate was consumed. Every experiment was repeated several times. Obtained initial velocities were used to calculate K_m and V_{max} using an iteration procedure on a microcomputer.

For peptidase assays 0.5 μg of the purified enzymes were incubated in the same way as described above with 100 μM of several substrates specific for chymotryptic or tryptic activity. In the case of Z-Leu-Leu-Glu-β-naphthylamine, the fluorescence emission was detected at 410 nm, whereas the excitation wavelength was fixed at 335 nm.

2.9. Molecular mass determination by native PAGE and 2D electrophoresis

The apparent molecular masses of the different proteasomes were determined by using the Pharmacia High Molecular Weight Calibration Kit on a non-denaturing PAGE (5–15% polyacrylamide gradient in Tris-HCl pH 8.8, according to Laemmli [22]). All electrophoretic runs were performed at 4°C starting at 20 mA for 75 min before continuing for 3, 8 or 20 h at 25 mA. After 5 h the running buffer was exchanged. Protein bands were visualized by Coomassie Blue staining. To obtain the apparent molecular masses, the relative migration values (R_f) for the individual proteasomes were calculated using a calibration curve.

For 2D gel electrophoresis, the non-denaturing gel was overlaid with 5 ml of 100 μM Suc-LLVY-AMC in assay buffer for 10 min at 37°C followed by a 30 s wash with water. Proteasome bands were detected in transillumination at 360 nm, excised and applied to denaturing SDS-PAGE.

2.10. Electron microscopy and image processing

Electron microscopy and image analysis of proteasome samples negatively stained with uranyl acetate was performed as described in detail elsewhere [23]. The data sets were subjected to image classification by means of correspondence analysis [24,25] before averaging.

3. Results

3.1. Coexpression of the α- and β-subunit genes

The expression system described in Section 2 allowed us to coexpress the four genes encoding α_1, α_2, β_1 and β_2 very efficiently. We first investigated whether constructs, in which all possible combinations of one α- and one β-gene were tandemly arranged, would yield fully assembled and proteolyti-

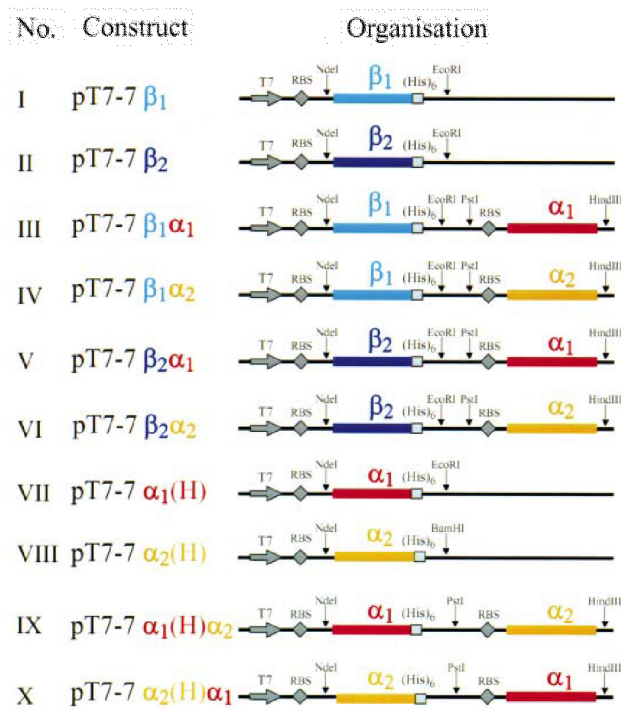

Fig. 2. Expression constructs used in structural and functional studies.

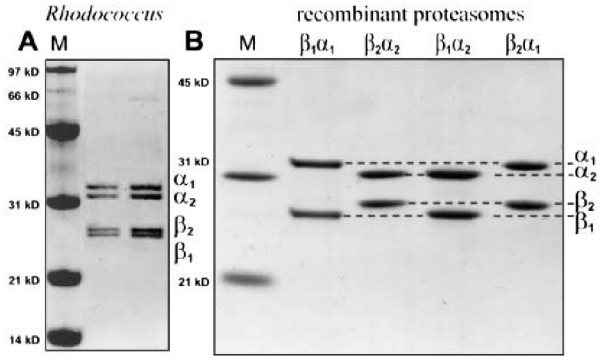

Fig. 3. 16% Tricine SDS-PAGE analysis of proteasome preparations; protein was visualized by Coomassie staining. (A) Purified proteasomes from *Rhodococcus*. The four bands correspond to the four subunits α_1, α_2, β_2 and β_1. (B) The subunit composition of the four different recombinant proteasomes from *Rhodococcus* expressed in *E. coli*. All recombinant proteins were purified using an Ni-NTA affinity column as described in Section 2.

cally active assembly products. To this end, we transformed *E. coli* BL21(DE3) cells with the appropriate plasmids, induced expression with IPTG, and directly loaded the cell lysate on a Ni-NTA affinity column. Recombinant proteins were eluted with an imidazole gradient after washing out non-specifically bound proteins. The yield of purified protein was approx. 5 mg per l of culture medium. Although in all constructs only the β-subunits carry the $(His)_6$ tag, both subunits (α and β) appear in approximately equimolar amounts in Tricine SDS-PAGE, indicating that they form a complex (Fig. 3). The existence of high molecular mass complexes, almost identical in size and shape to proteasomes isolated from *Rhodococcus*, was confirmed by native PAGE and electron microscopy (Figs. 4 and 5). The activity of the recombinant proteasomes was monitored by means of the fluorogenic peptide Suc-Leu-Leu-Val-Tyr-AMC. All four combinations of the α- and β-genes ($\alpha_1\beta_1$; $\alpha_2\beta_2$; $\alpha_1\beta_2$; $\alpha_2\beta_1$) behaved the same way, i.e. they yielded fully assembled and proteolytically active recombinant proteasomes (Figs. 3–5). Electron micrographs of proteasomes isolated from *Rhodococcus* and of the four recombinant forms were virtually identical and also the averages obtained from side views did not reveal any significant differences.

3.2. Expression of α-subunits

In order to examine whether α-subunits alone were able to assemble into homooligomeric rings, as had been observed with *Thermoplasma* subunits [11], we expressed α_1 and α_2 separately (constructs VII and VIII) and in combination (constructs IX and X). Although the two proteins were expressed and could be purified (Fig. 6A), we were able to detect neither any assembly products on native PAGE nor ring-shaped structures on electron micrographs. We conclude that the *Rhodococcus* α-subunits are not capable of assembling in the absence of β-subunits.

3.3. Expression of β-subunits

The proteolytically active β-subunits in eukaryotes and in archaea contain a propeptide which is cleaved off in the course of the assembly process [11,12]. This exposes a conserved threonine residue, whose OH group is thought to act as the catalytic nucleophile [9,10]. The β-subunits of the *Rhodococcus* proteasome contain unusually long propeptides (65 residues in β_1 and 59 residues in β_2). In the coexpression experiments described above (constructs III–VI) the β-subunits were correctly processed, thus yielding active proteasomes. Experiments with *Thermoplasma* proteasomes had previously shown that processing of the β-subunits is an autocatalytic process triggered by the α-subunits [11,12]. Obviously both *Rhodococcus* α-subunits can interact productively with both β-subunits and support their posttranslational processing. To rule out that in *Rhodococcus* the processing and activation of the β-subunit precursor is independent of the presence of α-subunits, we have analysed the two β-subunits expressed alone. As expected, posttranslational processing of the β-subunits does not occur, as indicated by their mobility in SDS-PAGE and confirmed by N-terminal sequencing. Under these conditions only the initiator methionine is removed and some non-specific degradation products are observed (Fig. 6B). All the cleavage sites in these degradation products are located within the propeptide sequence, but none corresponds to a correctly processed mature protein. We have found no indication, either by native PAGE or by electron microscopy, that the β-subunits are capable of forming ordered higher molecular mass assemblies. As expected, the β-subunits showed no measurable proteolytic activity.

3.4. Size and shape of Rhodococcus proteasomes

In order to determine the molecular masses of the *Rhodococcus* proteasomes and the various recombinant proteasomes more accurately, we subjected them to pore gradient electrophoresis. Provided that the influence of the electrical charge of a protein can (largely) be eliminated, the decreasing pore size in a gradient gel will increasingly restrict the migration of a protein and thus the position of a protein band is a measure of its size [26]. Fig. 4 shows the migration behaviour of *Rhodococcus* proteasomes and of the various recombinant α+β constructs on a 5–15% pore gradient gel after electrophoresis for 9 h 45 min. For the sake of comparison, we performed electrophoretic runs over periods of more than 20 h. No differences in the migration patterns were visible, indicating that the migration rates had approached zero. Based on the migration pattern of several reference proteins, amongst them the

Table 1
Comparison of experimentally determined and theoretically calculated molecular masses

	Rhodococcus	$\beta_1\alpha_1$	$\beta_2\alpha_2$	$\beta_1\alpha_2$	$\beta_2\alpha_1$
Molecular mass determination by native PAGE	718	749	712	693	756
Theoretical molecular mass for 7-fold symmetry	731	745	739	739	745
Theoretical molecular mass for 6-fold symmetry	626	639	633	633	639

The molecular masses (in kDa) were calculated as described in Section 2. The theoretical molecular masses were derived from the protein sequences of the four subunits assuming either a 6-fold or a 7-fold symmetry of the complex.

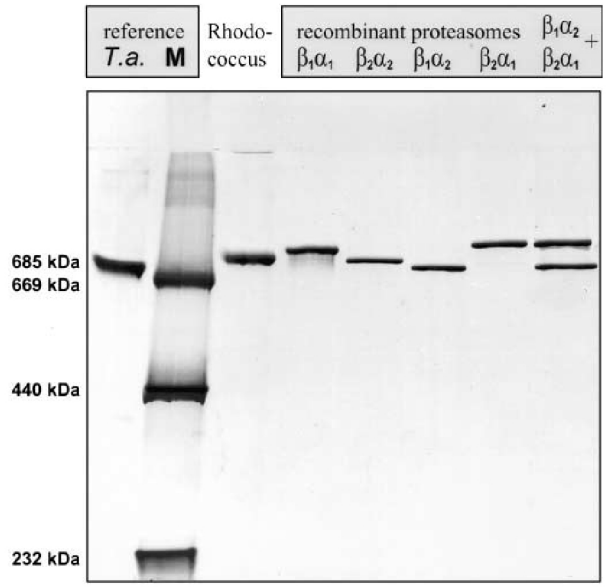

Fig. 4. Pore gradient electrophoresis using a non-denaturing 5–15% polyacrylamide gradient gel in Tris-HCl pH 8.8 [22]. The electrophoretic run was performed at 4°C as described in Section 2. Protein bands were visualized by Coomassie staining. For reference, the HMW Calibration Kit (Pharmacia) and *Thermoplasma* proteasomes (685 kDa) were used. In the last lane, two different recombinant proteasomes ($\beta_1\alpha_2$ and $\beta_2\alpha_1$) were mixed.

Thermoplasma 20S proteasome, we calculated the molecular masses of each type of proteasome (Table 1). The migration behaviour of the *Thermoplasma* proteasome did not deviate from the molecular size-molecular mass relationship of the other protein standards, and was in good agreement with its theoretical molecular mass of 685 kDa. The first and most important result of the pore gradient electrophoresis was that the proteasomes isolated from *Rhodococcus* as well as the four recombinant α+β proteasomes gave a single sharp band. We checked by means of SDS-PAGE that the single band obtained with *Rhodococcus* proteasomes contained all four subunits (data not shown). With mixtures of two types of proteasomes (e.g. $\alpha_2\beta_1$ plus $\alpha_1\beta_2$) we were able to resolve them in two separate bands. Hence we can rule out that in *Rhodococcus* two distinct subpopulations of proteasomes exist. In Table 1 we compared the experimentally determined molecular masses of the five types of *Rhodococcus* proteasomes with the theoretical values derived from the protein sequences of the four subunits ($\alpha_1 = 28.3$ kDa, $\alpha_2 = 27.8$ kDa, $\beta_1 = 24.2$ kDa, $\beta_2 = 24.1$ kDa) assuming a stoichiometry of $\alpha_{6\times}\beta_{6\times}\beta_{6\times}\alpha_{6\times}$ or $\alpha_{7\times}\beta_{7\times}\beta_{7\times}\alpha_{7\times}$, i.e. assuming either 6-fold or 7-fold symmetry. Obviously, in all five cases the experimentally determined molecular mass is in better agreement with 7-fold than with 6-fold symmetry.

The electron micrographs indicate that the proteasomes isolated from *Rhodococcus* as well as the four recombinant species all have the same structure. The averages derived from side views are all very similar to each other and they clearly resemble side views obtained from *Thermoplasma* proteasomes. In principle, it should be possible to determine the symmetry of proteasomes in an unambiguous manner from end views, i.e. projections down the symmetry axis. In practice, this is notoriously difficult and prone to errors with assemblies composed of several rings stacked together and not being in register (see e.g. [23,27]). Even small tilts of the cylinder axis with respect to the normal cause severe distortions in the projection images. Nevertheless, we have subjected side views to image analysis procedures, including eigenvector-eigenvalue analysis and classification. In data sets of proteasomes from *Rhodococcus*, 7-fold eigenvectors were clearly predominant but the class averages were not unambiguous, i.e. they showed some deviation from strict 7-fold symmetry. With all four recombinant proteasomes we found 6-fold and 7-fold eigenvectors amongst the first five eigenimages. We were able to separate the data set into classes with close-to-6-fold and close-to-7-fold symmetry. As an example, we give the statistics for the top views of the $\alpha_1\beta_2$ complex: of the 2045 individual molecules examined 45% showed 7-fold symmetry, 17% showed 6-fold symmetry and 24% remained unassigned, i.e. they were in between the two symmetries. The rest of the data set (14%) were distorted molecules.

3.5. Substrate specificity and kinetic parameters

We compared the substrate specificities of the proteasomes isolated from *Rhodococcus* and of the four recombinant species using fluorogenic peptides (Table 2). The progress of substrate hydrolysis was monitored continuously. With all five species we found the highest specific activity against the 'chymotryptic' substrate Suc-Leu-Leu-Val-Tyr-AMC. With Suc-Ala-Ala-Phe-AMC and Z-Gly-Gly-Leu-AMC the activity was much lower and for the small dipeptide Suc-Leu-Tyr-AMC the activity was in all cases of the proteasome species two to three orders of magnitude lower. Surprisingly, a small but not negligible specific activity was found for the 'tryptic' peptide Boc-Leu-Arg-Arg-AMC. Although this pattern of activities is the same for the set of peptides used as substrates, there are significant differences between the various proteasome species in their specific activity for any single substrate. Against Suc-Leu-Leu-Val-Tyr-AMC, the recombinant $\beta_2\alpha_1$ proteasome shows a 4-times higher specific activity than the proteasome isolated from *Rhodococcus* or the $\beta_1\alpha_1$ proteasome. In these experiments it was assumed that all proteasomes were active, i.e. that protein concentration meant active enzyme. We have no indication that this might not be the case; certainly propeptide removal was quantitative in all constructs and in *Rhodococcus* proteasomes.

Building upon the results of the peptidase assays, we measured the kinetic parameters of Suc-Leu-Leu-Val-Tyr-AMC

Table 2
Comparison of the substrate specificities of proteasomes isolated from *Rhodococcus* and recombinant proteasomes

Substrate	$\beta_2\alpha_1$	$\beta_2\alpha_2$	$\beta_1\alpha_2$	$\beta_1\alpha_1$	*Rhodococcus*
Suc-Leu-Leu-Val-**Tyr**-AMC	2136	913	1648	472	578
Suc-Ala-Ala-**Phe**-AMC	365	280	218	126	72
Z-Gly-Gly-**Leu**-AMC	197	160	49	28	29
Suc-Leu-**Tyr**-AMC	1.4	n.d.	n.d.	0.8	0.76
Boc-Leu-Arg-**Arg**-AMC	6.5	6.4	3.6	1.4	2.5
Z-Ala-Arg-**Arg**-AMC	0.3	n.d.	n.d.	n.d.	n.d.
Bz-Val-Gly-**Arg**-AMC	1.5	n.d.	n.d.	n.d.	n.d.

All peptidase assays were performed at 37°C using 0.5 μg of the purified enzymes as described in Section 2. Every experiment was repeated three times. Values for specific activities (in μmol min^{-1} mg^{-1}) were corrected with the corresponding values of the negative controls. n.d., not determined.

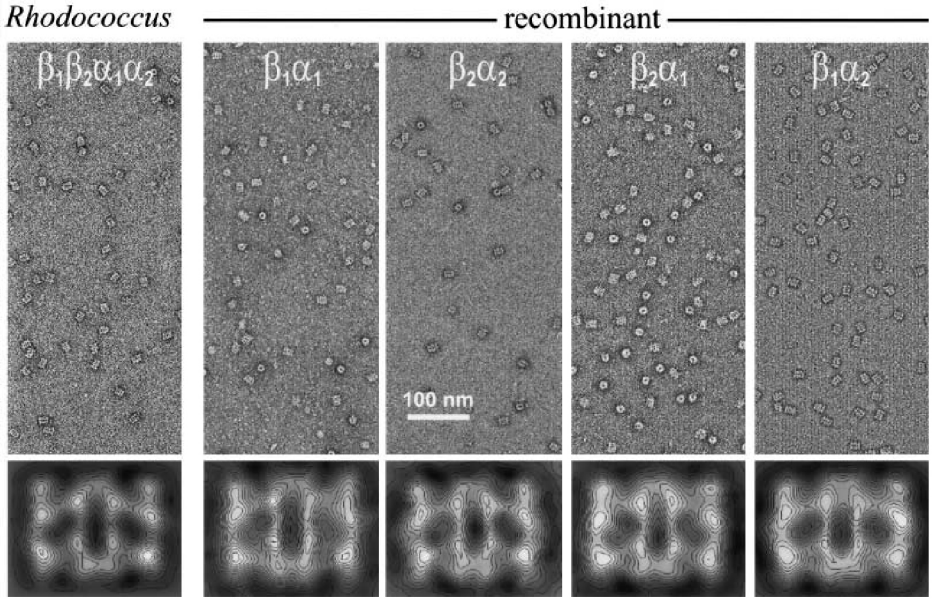

Fig. 5. Electron micrographs of isolated and recombinant *Rhodococcus* proteasomes with corresponding averages of the side views (bottom).

hydrolysis. Continuous measurements and calculation of the K_m values were carried out as described in Section 2 (Table 3). The K_m values measured for both constructs containing the β_2 subunit were lower than for those containing the β_1 subunit. It is also interesting to note that the exchange of the α-subunits has a significant effect on both β-subunits. Most surprisingly, the proteasome isolated from *Rhodococcus* has a K_m value of 125 μM which is 1.5–2-times higher than the K_m values of all four recombinant proteasomes.

4. Discussion

It is remarkable that both α-subunits of the *Rhodococcus* proteasome can interact with both β-subunits to form fully assembled and proteolytically active complexes. Obviously, the two operons encoding $\beta_1\alpha_1$ and $\beta_2\alpha_2$, respectively, have not yet diverged to an extent that would prevent a productive interaction. The kinetic constants (Table 3) of the four two-subunit constructs ($\beta_2\alpha_1$, $\beta_2\alpha_2$, $\beta_1\alpha_2$, $\beta_1\alpha_1$) are rather similar. Minor, but significant differences exist, indicating for example that the exchange of α_1 and α_2 has an effect on turnover rates although the α-subunits are not directly involved in the cleavage of substrate. They have a role, however, in controlling the accessibility of the central proteolytic cavity and, perhaps, in the translocation of substrate to the active sites.

The experiments reported in this communication indicate that there are important differences in the assembly pathways between archaeal and bacterial proteasomes. Unlike *Thermoplasma*, where the α-subunits assemble spontaneously into seven-membered rings which seem then to act as a template for the assembly of the β-subunits [11], the α-subunits from *Rhodococcus* are not capable of self-assembly. Neither α_1 or α_2 nor both α-subunits together form higher-order structures. As in *Thermoplasma*, the autocatalytic processing of the *Rhodococcus* β-subunit is dependent on the presence of α-subunits; both α-subunits support processing of both β-subunits. The length of the prosequences of β_1 (65 residues) and β_2 (59 residues) suggests that they may have other functions in addition to preventing premature activation of the β-subunits. It is interesting to note that the prosequences of β_1 and β_2 are much more divergent (68% identity) than the mature subunits (86% identity). The multiple cleavages observed in the β-subunits prosequences may be taken as an indication that they do not fold into a very compact structure.

With regard to the four models which we originally envisaged for the subunit topology of the *Rhodococcus* proteasome, we can, based on the experimental data reported in this communication, rule out several of them. Although electron microscopy and image analysis of end-on views failed to produce an unequivocal answer, there are several lines of evidence strongly in favour of a 7-fold or pseudo-7-fold symmetry. Averages of the side views correspond very closely to side

Table 3
Determination of the kinetic parameters for the hydrolysis of Suc-Leu-Leu-Val-Tyr-AMC by isolated and recombinant *Rhodococcus* proteasomes

	Recombinant proteasomes				*Rhodococcus*
	$\beta_2\alpha_1$	$\beta_2\alpha_2$	$\beta_1\alpha_2$	$\beta_1\alpha_1$	$\beta_1\beta_2\alpha_1\alpha_2$
K_m (μM)	61.4±3.5	66.4±2.2	71.2±2.1	84.3±2.9	125±7.6
V_{max} (nmol/s)	28.51	12.75	23.04	7.2	11.00

Measurements were performed at 37°C. 0.5 μg of the purified enzymes were added to several substrate concentrations (10–1000 μM) and the reactions were monitored by the increase of fluorescence emission as described in Section 2. The kinetic parameters were calculated from the initial velocities using an iteration procedure.

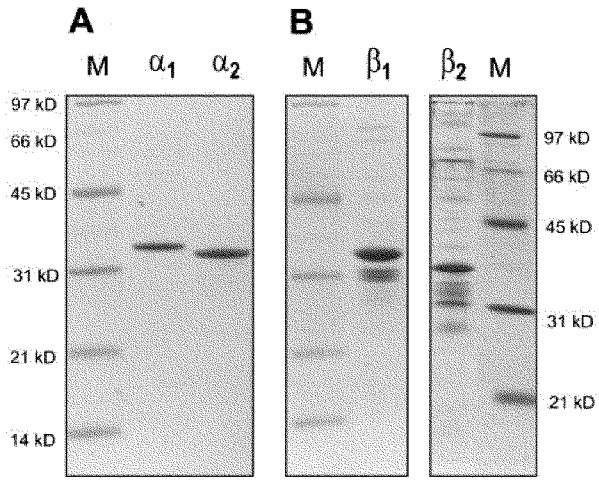

Fig. 6. (A) 16% Tricine SDS-PAGE of purified α_1- and α_2-subunits expressed in the absence of β-subunits. No degradation products were observed. (B) Tricine SDS-PAGE of recombinant β-subunits. In both cases the main band corresponds to the unprocessed β-precursors. Additionally, some non-specific degradation products are observed. N-terminal sequencing showed that all cleavage sites were within the prosequence (−48 to −18).

views of the *Thermoplasma* proteasome where the 7-fold symmetry is firmly established [28,29]. The apparent molecular masses of the various constructs determined by pore gradient electrophoresis are consistently closer to the theoretical molecular masses that assume 7-fold symmetry than to those assuming 6-fold symmetry. Hence, we conclude that the *Rhodococcus* proteasome, unlike the proteasome-related HslV protease found in other eubacteria, has seven-fold symmetry. This rules out model III, where the strict alternation of subunits would implicate an even-numbered symmetry. We can also rule out model I, which suggests that two distinct subpopulations might coexist, reflecting the pairwise arrangement of the four genes in the two operons. The pore gradient electrophoresis has a sufficiently good resolution to discriminate between the four α+β constructs which differ in theoretical molecular masses by only 6 kDa. Moreover, when the products of two constructs are mixed together, two well separated bands are observed. Proteasomes isolated from *Rhodococcus*, however, yield a single sharp band. We, therefore, conclude that a single population of proteasomes exists which is built from all four subunits. Additionally, it is interesting to note that the kinetic constants of proteasomes isolated from *Rhodococcus* are quite different from those measured for the four two-subunit constructs (see Table 3). For a mixture of two distinct subpopulations one would expect a K_m that lies in between the K_m values of the two species. Obviously, the interaction of the two β-subunits in the $\beta_1\beta_2\alpha_1\alpha_2$ complexes generates a significant change in cooperativity. Given the few amino acid exchanges between the two β-subunits, especially in the N-terminal half of the molecule, which is involved in active site formation, this is a surprising finding. By stepwise back-mutation of β-subunits it should be feasible to identify those residues which are critically involved in generating this change in cooperativity.

At present we are not in a position to discriminate between models II and IV. Both models assume that all four subunits were incorporated into a single proteasome, but while model IV allows the subunits to take random positions in their respective α- or β-rings, model II suggests that they segregate into four homooligomeric rings. Although our studies with recombinant constructs show that both α-subunits can productively interact with both β-subunits, this cannot be considered as conclusive evidence in favour of model IV. A kinetic partitioning, which might be mediated by the β-subunit prosequences, could lead to a segregation into homooligomeric rings. A role of the prosequences in determining the pattern of subunit interactions was proposed previously for eukaryotic proteasomes [30] which, unlike *Thermoplasma* proteasomes, cannot be reconstituted in vitro after dissociation. We are currently establishing an in vitro reconstitution system for the *Rhodococcus* proteasome which will allow us to clarify further these issues.

Acknowledgements: We thank M. Boicu for DNA sequencing, J. Kellermann for protein sequencing and Ute Santarius for electron microscopy. These studies were supported by a grant from the Human Frontier Science Program to W.B.

References

[1] Wenzel, T. and Baumeister, W. (1995) Nature Struct. Biol. 2, 199–204.
[2] Lupas, A., Koster, A.J. and Baumeister, W. (1993) Enzyme Protein 47, 252–273.
[3] Peters, J.M., Cejka, Z., Harris, J.R., Kleinschmidt, J.A. and Baumeister, W. (1993) J. Mol. Biol. 234, 932–937.
[4] Coux, O., Tanaka, K. and Goldberg, A.L. (1996) Annu. Rev. Biochem. 65, 801–847.
[5] Stock, D., Nederlof, P., Seemüller, E., Baumeister, W., Huber, R. and Löwe, J. (1996) Curr. Opin. Biotechnol. 7, 376–385.
[6] Lupas, A., Zwickl, P., Wenzel, T., Seemüller, E. and Baumeister, W. (1995) Cold Spring Harbor Symp. Quant. Biol. 60, 515–524.
[7] Hilt, W. and Wolf, D. (1996) Trends Biochem. Sci. 21, 96–102.
[8] Dahlmann, B., Kopp, F., Kuehn, L., Niedel, B., Pfeifer, G., Hegerl, R. and Baumeister, W. (1989) FEBS Lett. 251, 125–131.
[9] Löwe, J., Stock, D., Jap, B., Zwickl, P., Baumeister, W. and Huber, R. (1995) Science 28, 533–539.
[10] Seemüller, E., Lupas, A., Stock, D., Löwe, J., Huber, R. and Baumeister, W. (1995) Science 268, 579–582.
[11] Zwickl, P., Kleinz, J. and Baumeister, W. (1994) Nature Struct. Biol. 1, 765–769.
[12] Seemüller, E., Lupas, A. and Baumeister, W. (1996) Nature 382, 468–470.
[13] Dahlmann, B., Kopp, F., Kuehn, L., Hegerl, R., Pfeifer, G. and Baumeister, W. (1991) Biomed. Biochim. Acta 50, 465–469.
[14] Zwickl, P., Grziwa, A., Pühler, G., Dahlmann, B., Lottspeich, F. and Baumeister, W. (1992) Biochemistry 31, 964–972.
[15] Lupas, A., Zwickl, P. and Baumeister, W. (1994) Trends Biochem. Sci. 19, 533–534.
[16] Rohrwild, M., Coux, O., Huang, H.-C., Moerschell, R.P., Yoo, S.J., Seol, J.H., Chung, C.H. and Goldberg, A.L. (1996) Proc. Natl. Acad. Sci. USA 93, 5808–5813.
[17] Tamura, T., Nagy, I., Lupas, A., Lottspeich, F., Cejka, Z., Schoofs, G., Tanaka, K., De Mot, R. and Baumeister, W. (1995) Curr. Biol. 5, 766–774.
[18] Schägger, H. and von Jagow, G. (1987) Anal. Biochem. 166, 368–379.
[19] Bradford, M.M. (1976) Anal. Biochem. 72, 249–254.
[20] Nagy, I., Schoofs, G., Vanderleyden, J. and De Mot, R. (1996) DNA Seq. (in press).
[21] Tabor, S. and Richardson, C. (1985) Proc. Natl. Acad. Sci. USA 82, 1074–1078.
[22] Laemmli, U.K. (1970) Nature 227, 680–685.
[23] Baumeister, W., Dahlmann, B., Hegerl, R., Kopp, F., Kuehn, L and Pfeifer, G. (1988) FEBS Lett. 241, 239–245.
[24] Van Heel, M. and Frank, J. (1981) Ultramicroscopy 6, 187–194.
[25] Frank, J. and van Heel, M. (1982) J. Mol. Biol. 161, 134–137.

[26] Andersson, L.-O., Borg, H. and Mikaelsson, M. (1972) FEBS Lett. 20, 199–202.
[27] Marco, S., Urena, D., Carrascosa, L., Waldmann, T., Peters, J., Hegerl, R., Pfeifer, G., Sack-Kongehl, H. and Baumeister, W. (1994) FEBS Lett. 341, 152–155.
[28] Jap, B., Pühler, G., Lücke, H., Typke, D., Löwe, J., Stock, D., Huber, R. and Baumeister, W. (1993) J. Mol. Biol. 234, 881–884.
[29] Pühler, G., Weinkauf, S., Bachmann, L., Müller, S., Engel, A., Hegerl, R. and Baumeister, W. (1992) EMBO J. 11, 1607–1616.
[30] Schauer, T.M., Nesper, M., Kehl, M., Lottspeich, F., Muller, T.A., Gerisch, G. and Baumeister, W. (1993) J. Struct. Biol. 111, 135–147.